Annual variability and regulation of methane and sulfate fluxes in Baltic Sea estuarine sediments

Joanna E. Sawicka and Volker Brüchert

Department of Geological Sciences, Stockholm University, Stockholm, 10691, Sweden

Correspondence to: Volker Brüchert (volker.bruchert@geo.su.se)

Abstract. Marine methane emissions originate largely from near-shore coastal systems, but emission estimates are often not based on temporally well-resolved data or sufficient understanding of the variability of methane consumption and production processes in the underlying sediment. The objectives of our investigation were to explore the effects of seasonal temperature, changes in benthic oxygen concentration, and historical eutrophication on sediment methane concentrations and benthic fluxes at two type localities for open-water coastal versus eutrophic, estuarine sediment in the Baltic Sea. Benthic fluxes of methane and oxygen, sediment porewater concentrations of dissolved sulfate, methane, and ^{35}S-sulfate reduction rates were obtained over a 12-month period from April 2012 to April 2013. Benthic methane fluxes varied by factors of 5 and 12 at the offshore coastal site and the eutrophic estuarine station, respectively, ranging from 0.1 mmol $m^{-2}d^{-1}$ in winter at an open coastal site to 2.6 mmol $m^{-2}d^{-1}$ in late summer in the inner eutrophic estuary. Total oxygen uptake (TOU) and ^{35}S-sulfate reduction rates (SRR) correlated with methane fluxes showing low rates in the winter and high rates in the summer. The highest porewater methane concentrations also varied by factors of 6 and 10 over the sampling period with lowest values in the winter and highest values in late summer-early autumn. The highest porewater methane concentrations were 5.7 mM a few centimeters below the sediment surface, but never exceeded the in-situ saturation concentration. 21 – 24% of the total sulfate reduction was coupled to anaerobic methane oxidation lowering methane concentrations below the sediment surface far below the saturation concentration. The data imply that bubble emission likely plays no or only a minor role for methane emissions in these sediments. The changes in porewater methane concentrations over the observation period were too large to be explained by temporal changes in methane formation and methane oxidation rates due to temperature alone. Additional factors such as regional and local hydrostatic pressure changes and coastal submarine groundwater flow may also affect the vertical and lateral transport of methane.

Keywords Methane cycling, coastal and estuarine sediment, seasonality

1 Introduction

The world's estuaries have been suggested to emit between 1.8 and 6.6 Tg CH_4 y^{-1} to the atmosphere (Borges and Abril, 2011; Amouroux et al 2002, Marty et al., 2001; Middelburg et al., 2002; Sansone et al., 1999; Upstill-Goddard et al., 2000), a considerable portion of the estimated total oceanic emissions of 10-30 Tg CH_4 y^{-1} (Judd, 2004; Etiope et al., 2008; Kirschke et al., 2013). As other globally upscaled estimates of emissions, these estimates also have considerable uncertainties. In the case of estuaries, a major cause of the uncertainty are relatively few spatially and temporally resolved measurements of anaerobic carbon degradation measurements in sediments and measurements of methane fluxes from sediments. In estuarine waters methane can be derived from underlying anoxic sediments, transported laterally due to freshwater or sewage discharge, seepage of methane-rich groundwater, or it can be derived from near-shore aquatic plants (Borges and Abril, 2011). The amount of sedimentary methane production in estuaries is a function of organic matter availability, bottom water oxygen concentrations, and the salinity of the estuary. Methane production is generally greater in low-salinity estuaries because of lower sulfate availability to promote bacterial sulfate reduction (Borges and Abril, 2011). Methane fluxes from estuarine sediments are characterized by significant spatial and temporal variability (Borges and Abril 2011). Temporal patterns show that concentrations and fluxes of CH_4 are generally higher in the warmer season and low in the colder season (Crill et al., 1983, Martens and Klump, 1984, Musenze et al., 2014; Reindl and Bolałek, 2014). Notably, very few studies have considered CH_4 fluxes in high-latitude environments during snow- and ice-covered periods. While shallow systems within the tidal range derive a significant amount of the methane flux from ebullition (Martens and Klump, 1984), groundwater discharge, tidal pumping, and transport by aquatic plants (Middelburg et al., 2002; Kristensen et al 2008), the transport from deeper systems such as fjords and fjärds is thought to occur largely by molecular diffusion (Abril and Iversen, 2002, Sansone et al., 1998).

Globally more than 90% of methane produced in marine sediments is estimated to be oxidized by the anaerobic oxidation of methane (AOM), mostly in the sulfate-methane transition zone (Knittel and

Boetius, 2009, Martens and Berner, 1974; Jørgensen and Parkes, 2010). It is not known how much methane is oxidized by AOM in estuarine sediments. In addition, up to 90% of the remaining methane that reaches the sediment surface may be oxidized aerobically at the sediment surface or in the water column (Reeburgh, 2007). Yet, methane concentrations in estuarine waters are almost always higher than the atmospheric equilibrium concentration indicating that microbial oxidation processes and physical exchange with the atmosphere in estuaries are relatively inefficient in removing methane. Despite its obvious importance, only few studies have specifically addressed anaerobic oxidation of methane by sulfate and aerobic oxidation in estuarine environments (e.g., Treude et al., 2005, Thang et al., 2013).

The objective of this study was therefore to further elucidate mechanisms behind temporal variability of methane fluxes in a high-latitude coastal and estuarine environment with strong seasonal temperature variability, winter ice cover, and variable degree of eutrophication stress. These data fill an important gap of global inventories of nearshore sediment methane dynamics and help improve our mechanistic understanding of methane emissions from marine near-shore systems. We determined porewater concentrations of methane and sulfate, measured sulfate reduction rates with the ^{35}S-sulfate tracer method, and conducted core incubations to determine benthic fluxes of methane and oxygen at two deep stations of a low-salinity Baltic Sea estuary inside and at the opening of the estuary to the Baltic. Investigations were carried out over four seasons to capture the annual variability of chemical and biological conditions at the sediment surface and their influence on methane dynamics.

2 Materials and methods

2.1 Site description

Himmerfjärden (Figure 1) is a fjord-type estuary with a surface area of 174 km^2, a volume of 2968 x 10^6 m^3, and a N-S bottom water salinity gradient increasing from 5.5‰ in the inner part to 7.0‰ at the opening to the Baltic. It is morphologically characterized by four basins, divided by sills

and has a low flushing rate of about 0.025/day (Savage and Elmgren, 2010). The freshwater discharge is small compared to the exchange with the open Baltic and was estimated to be 23 m^3/s on average in 2012 comprising land run-off and precipitation (30% and 21%, respectively), outflow from Lake Mälaren from the north (19%) and the river Trosaån (23%), and discharge from a sewage treatment plant (6%) (Larsson et al., 2012). The sewage treatment plant, built in the early 1970s, treats sewage water from ca. 314,000 inhabitants of the southern Stockholm metropolitan area, and its inorganic effluent is discharged mainly in the form of inorganic nitrogen and phosphorus to the inner basins (Savage and Elmgren, 2010). In 2012, the sewage treatment contributed 45% of the total phosphorus and 57% of the total inorganic nitrogen discharge to the northern Himmerfjärden area (Larsson et al., 2012) and discharged 1676 tons carbon (measured as chemical oxygen demand COD) (Stridh, 2012). The estuary undergoes thermohaline stratification during late summer and autumn, especially in the inner part, which experiences regular seasonal bottom water hypoxia. The tidal range is low (few cm) and relatively cold bottom waters (1.5 - 9°C) dominate throughout the year. Water level can vary annually by about 50 cm depending on local wind and hydrographic conditions. Late-summer-early fall bottom water hypoxia has also been reported occasionally for the outer basins of the estuary, when winds are weak and circulation is inhibited (Elmgren and Larsson, 1997). Sedimentation areas in Himmerfjärden can be divided into accumulation and transport bottoms (Jonsson et al., 2003). About 21% of the sediment surface in Himmerfjärden is classified as accumulation bottoms of particulate material and receives 3.3-9 mol C m^{-2} y^{-1} (Thang et al., 2013; Karlsson et al., 2010).

Bottom water and sediment samples were taken from a station in the inner part of Himmerfjärden, Station H6, and from a station located outside the estuary, Station B1 (Figure 1). Samples were collected in April 2012, August 2012, and October 2012 with the research vessel R/V Limanda, and in February 2013 with the ice-breaking research vessel R/V Aurelia. In addition, in April 2013 whole-core incubations were performed to determine methane and oxygen fluxes to record a full year of seasonal variability. Station B1 has soft, olive grey, muddy sediment with a 1-2 cm-thick rusty brown surface layer that was present year round, while the sediment at station H6 is soft, laminated

131 black mud with a 1-2 mm thin brown surface layer that occurred only during the winter and spring.
132 Sediment accumulation rates range from 0.98 cm yr^{-1} in the innermost part of the estuary to 0.77 cm yr^{-1}
133 in the outer part of the estuary (Thang et al., 2013).
134
135 **2.2 Sample collection**
136 Sediments with well-preserved sediment surfaces were collected with a Multicorer in acrylic tubes (9.5
137 cm diameter) to 40 cm depth to determine ^{35}S-sulfate reduction rates, porosity, and the porewater
138 constituents methane and sulfate. Additional cores were collected for sediment core incubations.
139 Porewater methane samples were immediately collected on-board the research vessels R/V Limanda
140 and the ice-class vessel R/V Aurelia from the cores as described below. The other cores were capped
141 with rubber stoppers, transported to the marine laboratory on the island of Askö within 90 minutes and
142 kept cold at bottom water temperature for later experiments and subsampling. In February 2013, ice
143 partially covered Station B1 and there was complete ice cover at Station H6, and sampling was only
144 possible after ice breaking. For whole-core incubations, 30 l of bottom water was collected with a 5
145 liter HydroBios bottle and kept cold until for the experiments. Temperature, salinity, and oxygen
146 concentrations were determined with a handheld WTW Oxygen meter directly in the water overlying
147 the sediment cores.
148
149 **2.3 Organic carbon concentrations and porosity**
150 Concentrations of organic carbon were determined for the topmost cm of sediment on freeze-dried
151 sediment with a Fisons CHN elemental analyzer after treatment with 1M HCl to remove inorganic
152 carbon. Water content (%) was determined by drying 5 ml of sediment at 105°C and calculating the
153 percent loss after drying.
154

2.4 Methane analysis

Samples for methane were collected directly through the side of taped, pre-drilled core liners and taken in 2-cm intervals minutes after the core was retrieved on deck. The core sampling method used in this study permits complete sampling and preservation of porewater methane within 5 minutes after the core was on deck. Under these circumstances, loss of methane due to gas loss was low and methane concentrations could be determined for porewaters that were far above the saturation limit at 1 atmosphere pressure for the salinity and temperature range of the bottom water (between 1.9 mM and 2.4 mM). A sediment sample of 2.5 mL was taken with a 3 mL cut-off syringe. The sample was transferred to a 20 mL serum vial containing 5 mL 5 M NaCl and immediately closed with a thick septum and an aluminum crimp seal (Thang et al., 2013). For analysis, the sample was shaken and 5 mL of brine was injected into a sample vial to displace 5 mL gas out of a vial into the syringe. The CH_4 measurements were carried out on a gas chromatograph (GC) with a flame ionization detector (FID) (SRI 8610C) after separation on a 3 feet Porapak Q pre-column before a 9 feet Hayesep D column with N_2 as carrier gas. CH_4 standards 100 ppm, 1000ppm, and 10000 ppm (Air Liquide) were used for calibration.

The concentration of methane (mM) of a sample was calculated as follows:

$$CH_4(mM) = \frac{CH_{4\ hsp} \cdot V_{hsp}}{1000 \cdot 24.148 \cdot V_{sed} \cdot \rho} \quad (1)$$

where $CH_{4_{hsp}}$ is the concentration of methane in the headspace of the sample vial (ppm), V_{hsp} is the volume of the headspace (L), V_{sed} is the volume of the sediment sample (L), ρ is sediment porosity, and 24.148 (L mol^{-1}) is the molar volume of gas at standard pressure 100 kPa and 298 K. The reproducibility of the method has been tested at a station in the archipelago that is not part of this study by replicating methane sampling on multiple sediment cores. Concentrations in multiple cores deviated by about 15%.

2.5 Sulfate concentration

Porewater samples for sulfate concentration measurements were obtained using rhizones (Atlas Copco Welltech) (Seeberg-Elverfeldt et al 2005). Rhizones were treated for 2 hours in 2M HCl, followed by two rinses with deionized water for 2 hours and final storage in deionized water. Rhizones were connected to 10 mL disposable plastic syringes via 3-way luerlock stopcocks and inserted in 1-cm intervals through tight-fitting, pre-drilled holes in the liner of the sediment cores. The first mL of pore water was discarded from the syringe. No more than 2 ml were collected from each core to prevent cross-contamination of adjacent intervals (Seeberg-Elverfeldt et al., 2005). Sulfate concentrations were determined with a Dionex System IC 20 ion chromatograph. The detection limit for sulfate after twentyfold dilution to reduce the chloride peak size was 100 µM.

2.6 ^{35}S-Sulfate reduction rates

To determine bacterial sulfate reduction rates (SRR) sediment cores were subsampled in 40-cm long 28 mm-diameter cores with 1-cm spaced, silicon-sealed, pre-drilled small holes on the side for injections. For the incubation, the whole-core incubation method by Jørgensen (1978) was used. $^{35}SO_4^{2-}$ tracer solution was diluted in a 6 ‰ NaCl solution containing 0.5 mM SO_4^{2-}. 2.5 µl of the tracer solution (50kBq) was injected through the pre-drilled holes. The cores were then capped and sealed in plastic wrap foil and incubated for 8 hours at the respective bottom water temperatures. After this time, the incubations were stopped by sectioning the core in 1-cm intervals to 5 cm depth and in two centimeter intervals below this depth to the bottom of the core. Sediment sections were transferred to 50 ml plastic centrifuge tubes containing 20 ml zinc acetate (20% v/v) and shaken vigorously and frozen. The total amount of ^{35}S-labeled reduced sulfur (TRIS) was determined using the single-step cold chromium distillation method by Kallmeyer et al. (2004). TRIS and supernatant sulfate were counted on a TriCarb 2095 Perkin Elmer scintillation counter. The sulfate reduction rate was calculated using the following equation (Jørgensen, 1978):

$$^{35}SRR = \left(TRI^{35}S \Big/ (^{35}SO_4^{2-} + TRI^{35}S) \right) \cdot 1.06 \cdot SO_4^{2-} \cdot \rho \cdot 1/t \quad (2)$$

where SO_4^{2-} is the pore water sulfate concentration corrected for porosity ρ, $TRI^{35}S$ and $^{35}SO_4^{2-}$ are the measured counts (cpm) of total reduced inorganic sulfur species and sulfate, respectively, 1.06 is a correction factor accounting for the isotope discrimination of ^{35}S against ^{32}S-sulfate, and t is the incubation time. The sulfate reduction rate is reported as nmol cm^{-3} day^{-1}. Generally, when enough cores were available ^{35}SRR were measured on replicate cores for all depth intervals. The detection limit of the rate measurements accounting for distillation blanks and radioactive decay of ^{35}S between experiment and laboratory workup was 0.1 nmol cm^{-3} day^{-1}.

2.7 Whole-core sediment incubations

In order to account for the total benthic exchange of oxygen and methane by advection, diffusion, bioirrigation, and bioturbation, four intact cores with undisturbed sediment surfaces and clear overlying water were subsampled in the laboratory in acrylic tubes (i.d. 6.2 cm, height 25 cm) retaining about 10 cm of the overlying water. The sediment height in the tubes was approximately 10 cm. The cores were incubated in a 40-liter incubation tank filled with bottom water from the same station. Before the incubation the overlying water in the cores was equilibrated with bottom water in the tank. The overlying water in the cores was stirred by small magnetic bars mounted in the core liners and driven by an external magnet at 60 rpm. The cores were pre-incubated uncapped for 6 hours and subsequently capped and incubated for a period of 6 to 12 hours depending on the initial oxygen concentration in the bottom water.

2.7.1 Total oxygen uptake

Oxygen sensor spots (Firesting oxygen optode, PyroScience GmbH, Germany) with a sensing surface of 5 mm diameter were attached to the inner wall of two incubation cores (diameter 5.5 cm). The sensor spots were calibrated against O_2-saturated bottom water and oxygen-free water following the manufacturer's guidelines accounting for temperature and salinity of the incubation water. Measurements were performed with a fiberoptic cable connected to a spot adapter fixed at the outer core liner wall at the spot position. The O_2 concentration was continuously logged during incubations. Sediment total oxygen uptake (TOU) rates were computed by linear regression of the O_2 concentration over time.

2.7.2 Benthic methane fluxes

Benthic methane fluxes were determined from discrete water samples directly above the sediment-water interface and collected without headspace in 12 mL Exetainers (Labco, Wycombe, UK) prefilled with 50 µL of 50% $ZnCl_2$. Samples were collected at the beginning (time zero) and the end of the incubation (time final), usually after 24 hours. CH_4 concentrations were determined using the headspace equilibration technique (Kampbell et al., 1989) by replacing 3 ml of the water in the exetainers with high-purity helium gas at atmospheric pressure. The Exetainers were then shaken at 400rpm on a shaking table for 60 minutes to allow the gas to equilibrate between the headspace and the liquid phase and left to rest for half an hour. After equilibration 2.5 mL of NaCl brine was injected into an Exetainer to force the gas samples into an injection syringe while maintaining the headspace pressure. The samples were injected onto a 1 ml injection loop of a gas chromatograph (SRI 8610C) with FID detector using N_2 as carrier gas. CH_4 standards 5 ppm, 100 ppm and 1000 ppm (Air Liquide) were used to construct a calibration curve. The partial pressure of CH_4 in the equilibrated headspace and water was calculated using the solubility coefficient β for CH_4 using the salinity of the bottom water at the respective sample time (Table 1) (Wilhelm et al 1977), gas constant R (8.314 L kPa mol^{-1}

K^{-1}), air pressure P (kPa), headspace gas concentration $CH_{4\ hsp}$ (nmol), headspace volume (0.003L), water volume in the exetainer (0.009L), and laboratory temperature T (293 K) according to

$$CH_4\ (nM) = (CH_{4\ hsp} + \beta\ CH_{4\ hsp})^* P/RT \quad (3)$$

Fluxes (J) of CH_4 (mmol m^{-2} d^{-1}) during the whole core sediment incubations were calculated according to

$$J = (CH_{4\ start} - CH_{4\ end})/t * V/A \quad (4)$$

where $CH_{4\ start}$ and $CH_{4\ final}$ represent the end and start concentrations in mmol/m^3, V is headspace volume (m^3), A is the surface area of the incubation core (m^2), and t is the incubation time (days).

2.8 Diffusive flux calculations

Diffusive fluxes of methane and sulfate were estimated from the porewater gradients of methane and sulfate for the sediment surface and the sulfate-methane transition zone. Sediment cores at station B1 showed occasional burrows from deposit feeders in the topmost 2 cm of sediment, whereas sediment at station H6 was largely devoid of macro- and meiofauna. Since only one sample was taken from the topmost 2 cm, quantitative depth-related effects of bioturbation cannot be accounted for in this analysis and upward diffusive transport of methane was assumed as the dominant transport pathway. Fluxes were estimated using Fick's first law of diffusion

$$J = D_s \frac{dC}{dx} \quad (5)$$

assuming that flux was dominated by molecular diffusion, where dC is the change in concentration of dissolved sulfate (mM) or methane (mM) over a depth interval dx (cm), and D_s is the sediment diffusion coefficient calculated for the bottom water temperature and salinity according to Boudreau (1996). D_s was recalculated from the molecular diffusion coefficient D_o for sulfate and methane according to Iversen and Jørgensen (1994). Since the resolution of the porewater methane analysis was 2 cm, concentration changes below this resolution cannot be resolved. This could lead to an

overestimation of the flux across the sediment surface, e.g., due to aerobic methane oxidation in the topmost mm of sediment. Similar effects may occur in the sulfate-methane transition zone.

3. Results

3.1 Bottom water temperature, dissolved oxygen, sediment organic carbon

Over the observation period April 2012 through February 2013 bottom water salinity varied between 6.5 and 7.0‰ at station B1 and 5.4 and 6.5‰ at Station H6 (Table 1), while bottom water temperatures ranged from 2.4°C to 6.9°C for station B1 and 1.8°C to 9.4°C for station H6. The lowest and highest bottom water oxygen concentrations measured were 160 µM for station B1 and 40 µM for station H6 in April 2012, and 300 µM and 380 µM for station B1 and station H6 in February 2013, respectively. Surface sediment organic carbon concentrations were similar at the two stations ranging between 4.6 and 5.2% at Station B1, and 5.0% and 6.0% at Station H6 over the observation period.

3.2 Methane and sulfate concentrations

At both stations, the measured methane concentrations never exceeded the solubility limit for methane calculated for the *in situ* pressure, which ranged from 9.6 to 11.9 mM during the different sampling periods. At station B1, the highest methane concentrations in the sediment cores were recorded in October 2012, when they reached 0.9 mM (Figure 2a-d). Surprisingly, the lowest methane concentrations were recorded in August 2012. This was possibly due to drift of the vessel during sampling in rough seas at that time into an area underlain by neighbouring glacial clays with low porewater methane concentrations. Excluding the August data, methane concentrations were low and between 1 and 10 µM to a depth of 6 cm, 2 cm, and 6 cm in April, October, and February, respectively, before they increased sharply. At station H6, the highest and lowest concentrations in the cored depth interval were 5.7 mM and 1.5 mM, and recorded in August and February 2013, respectively. At this

station, the methane concentrations generally increased linearly from the surface down to 10 cm depth. Below this depth they only increased slightly or remained constant.

Sulfate concentration gradients changed between the different seasons at both stations reflecting changes in sulfate reduction rates over the observation period. At both stations, the sulfate concentration gradients were steepest in the topmost 8-10 cm in August, intermediate in April and October, and lowest in February indicating highest and lowest sulfate reduction rates in late summer and winter, respectively (Figure 2 a-h). At station B1, sulfate was never consumed completely and concentrations remained above 1.5 mM at the bottom of the core. In August and October, a distinct decrease in the sulfate concentration gradient occurred at around 8-10 cm depth. Despite some variability in the sulfate concentration profiles, the sulfate concentrations at the bottom of the core were similar during all observation periods. At station H6, sulfate always reached minimum detection concentrations of less than 100 µM in the cored sediment interval, albeit at substantially greater depth in February. The initial depth at which sulfate reached the lowest concentration from the surface down was defined as the initial minimum sulfate concentration depth, which occurred at 16 cm depth in April, 10 cm in August, 14 cm in October and at 25 cm depth in February.

3.3 ^{35}S-sulfate reduction rates

At Station B1, the depth-integrated SRR over the total core length varied from 0.5 to 2.3 mmol m^2 d^{-1}. The depth-resolved SRR ranged from 63 nmol cm^{-3} d^{-1} at the sediment surface to 0.2 nmol cm^{-3} d^{-1} at the bottom of the cored intervals (Figure 3 a-h, Table 2). Contrary to expectations, the lowest SRR were measured in August, which was possibly also due to the fact that the vessel drifted into a glacial clay area. The highest SRR were measured in the topmost 2 cm with the exception of October 2012, when the maximum was found at 3 cm depth. Below the depth of maximum SRR, rates decreased exponentially indicating that organoclastic sulfate reduction dominated and that the reactivity of the degrading organic material decreased exponentially with depth. More than 90% of the integrated sulfate reduction took place in the top 15 cm of sediment (Figure 5 a-d). Over the cored sediment

interval, there was no peak that could be attributed to significant AOM. Nevertheless, the distinct curvature of the methane concentration profile in February 2013 at station B1 suggests that methane was oxidized in the sulfate reduction zone and that some of the sulfate reduction may have been coupled to anaerobic methane oxidation.

At Station H6, depth-integrated SRR over the total core length varied from 9.2 to 11.7 mmol m^{-2} d^{-1}. The highest measured SRR was 338 nmol cm^{-3} d^{-1} and occurred at 2 cm depth in April 2012. Organoclastic sulfate reduction dominated the interval down to 10 cm. In April, August, and October 2012 two distinct sulfate reduction rate peaks were found at station H6, one at the surface, and a second peak between 10 cm and 18 cm depth. The latter peak covers the sulfate-methane transition zone and indicates that in this depth interval the rates of anaerobic methane oxidation coupled to sulfate reduction exceeded organoclastic sulfate reduction rates. We therefore defined the depth interval near the minimum sulfate concentration depth together with elevated SRR as the AOM zone (Table 2). Previous studies at nearby station H5 in Himmerfjärden also found AOM to be present at depths between 6 and 16 cm, which is in agreement with our findings (Thang et al., 2013; Wegener et al., 2012). The depth-integrated rates of SRR in the sulfate-methane transition zone at H6 were relatively constant over the three observation periods and varied between 2.4 mmol m^{-2} d^{-1} and 2.8 mmol m^{2} d^{-1} (Table 2). In February, however, when sulfate penetrated to 24 cm depth, sulfate reduction rates were about two times lower compared to the other months. The previously observed elevated rates between 10 and 18 cm depth were not visible, although another SRR peak was observed between 5 and 9 cm depth. However, the high concentrations of sulfate and low concentrations of methane in this depth interval in February make it unlikely that this peak is due to AOM. It is more likely that this peak is associated with organiclastic sulfate reduction, because no change in the sulfate or methane gradients was observed at this depth. Some sulfate reduction was also detected below 18 cm depth at station H6 in April, August, and October. Since non-radioactive carrier sulfate was added to the ^{35}S-tracer during these incubations, these rates indicate potential sulfate reduction activity in the methanogenic zone (Leloup et al., 2009).

3.4 Benthic exchange of oxygen, sulfate, and methane

Rates of total oxygen uptake are summarized in Table 2 and shown for comparison in Figure 4. Total oxygen uptake was lowest in February at both stations (B1: 12.0 ± 1.5 mmol m^{-2} d^{-1} and H6: 14.9 ± 1.6 mmol m^{-2} d^{-1}), and highest in August at station B1 (22.5 ± 2.9 mmol m^{-2} d^{-1}) and in April at station H6 (33.5 ± 3.5 mmol m^{-2} d^{-1}). Diffusive fluxes of sulfate from the water column into the sediment ranged from 0.2 mmol m^{-2} d^{-1} in February to 1.4 mmol m^{-2} d^{-1} in October at station B1, and from 1.3 mmol m^{-2} d^{-1} in February to 2.7 mmol m^{-2} d^{-1} in August at station H6 (Table 2). These rates are significantly lower than the depth-integrated radiotracer rates and indicate that sulfate is reoxidized below the sediment surface by reaction with reactive iron (Thang et al., 2013). Whole-core methane fluxes ranged from -0.1±0.05 mmol m^{-2} d^{-1} (February) to -1.2±0.6 mmol m^{-2} d^{-1} (August) at station B1 and from -0.3±0.1 mmol m^{-2} d^{-1} (April 2012) to -19.9±7.8 mmol m^{-2} d^{-1} (August) at station H6 (Figure 5, Table 2). However, the following year, a significantly higher methane flux of 3.9 mmol m^{-2} d^{-1} was measured in April 2013 at station H6. Significant upward diffusive methane fluxes ranged from 0.02 mmol m^{-2} d^{-1} (February 2012) to 0.3 mmol m^{-2} d^{-1} (August) at Station B1 and from 0.5 (February) to 2.3 mmol m^{-2} d^{-1} (August) at station H6. Thus, there was a generally poor agreement between whole-core and diffusive flux-derived methane fluxes. The large discrepancy between the August 2012 diffusive flux and whole-core flux is best explained that the cores were taken from sediments with different organic carbon contents. Since several Multicorer casts were taken per station and the vessel's positioning ability in strong winds was at best tens of meters, sediment heterogeneity can possibly explain this difference. The very high whole-core flux value measured in August 2012 at Station H6 is likely due to ebullition during the incubation at ambient air pressure and oversaturation of the porewater with respect to atmospheric pressure.

4. Discussion

4.1 Bottom water temperature and salinity

Correlations between biogeochemical rates and fluxes with bottom water temperatures in Himmerfjärden between April 2012 and February 2013 were weak for the period April-October, and forced by the low rates in the coldest observation period in early February 2013. All R values calculated for pairs of temperature versus rate/flux were less than 0.2 and not consistent for the fluxes of oxygen, methane, and sulfate indicating that additional environmental controlling factors played a role. It is likely that the microbial community involved in the cycling of methane and sulfur species in Himmerfjärden sediment is temperature-sensitive, and that the low rates in February 2013 are due to the 3°C temperature drop in bottom water from October 2012 to February 2013 (Table 1). This would be consistent with rate observations in comparable environments by Treude et al (2005a), Abril and Iversen (2002), Crill and Martens (1983), and Westrich and Berner (1988), and is also supported by studies of the microbial community composition of estuarine sediments that showed variations as a function of temperature (e.g., Zhang et al 2014). Regulation of methane fluxes largely by temperature implies that methane oxidation in Himmerfjärden sediment is less temperature-sensitive than methanogenesis preventing methane-oxidizing bacteria from keeping up with the enhanced methane flux during summer. This requires significantly higher temperature stimulation of methanogenesis than methane oxidation, the lack of an electron acceptor, or successful competition for the same electron acceptor by other organisms than methane-oxidizing bacteria. Publications from lake environments and terrestrial environments suggest that aerobic methane-oxidizing bacteria may indeed be less temperature-sensitive than methanogens (King, 1992; Wik et al., 2014; Nguyen et al., 2011). However, this argument is not directly applicable to marine habitats. In case of anaerobic methane oxidation, it is difficult to argue for a physiological temperature disadvantage of methane oxidizers compared to methanogens, because of the tight coupling between sulfate reduction and methane oxidation, the phylogenetic proximity of ANME to known methanogenic Archaea (Knittel and Boetius, 2009), and

similarities in membrane composition of ANME and methanogenic Archaea (Wegener et al., 2012). However, temperature control may not manifest itself by direct kinetic or bioenergetic regulation, but indirectly through the influence on competing processes, e.g., sulfate reduction and methanogenesis. Further, microbial community composition and biogeochemical rates often cannot be directly established from binary relationships with temperature, since other physical and chemical parameters such as salinity, bottom water oxygen concentrations, organic carbon accumulation also vary seasonally. Of these, salinity is not considered to be important for the present study, because the annual range in Himmerfjärden bottom water was only between 5.4 and 7 ‰, which is too small to affect the major electron acceptor and carbon degradation pathways.

4.2 Effects of organic matter composition and sedimentation

Organic carbon concentrations in Himmerfjärden are similar to other fjord- and fjärd-type estuarine sediments (Bianchi, 2007; Smith et al., 2015). Primary organic carbon export in Himmerfjärden varies strongly on both seasonal and interannual timescales (Blomqvist and Larsson, 1994). The major export periods occur during the spring phytoplankton bloom after ice breakup from March-April until early May, during a late-summer cyanobacterial bloom in August, and after a weaker, secondary phytoplankton bloom in September (Bianchi et al., 2002; Zakrisson et al., 2014; Harvey et al., 2015). Terrestrial-derived organic carbon that is not derived from the sewage treatment plant plays only a minor role in this system, because no major rivers enter the system and surface rainwater runoff is low. Based on sediment trap studies, the annual organic carbon flux in Himmerfjärden varies by more than an order of magnitude at station B1 and by about a factor of 3 in the inner parts of Himmerfjärden (Blomqvist and Larsson, 1994). Observations over a 5-year period by Blomqvist and Larsson (1994) indicated that primary organic carbon dominates organic sedimentation in the spring and summer at station B1, whereas station H6 is characterized by a spring term dominance of primary carbon deposition, but a much greater contribution of resuspended organic material to organic sedimentation during the fall (Blomqvist and Larsson, 1994).

A second effect to be considered is that stations B1 and H6 are located in bathymetric depressions. H6 is in the center of a sub-basin separated from the outer Himmerfjärd by a sill (Fig. 1). Likewise, Station B1 is located in a small depression at the head of a submarine channel that opens to the Baltic Sea. Fine-grained and reworked organic-rich material preferentially accumulates in these depressions (Jonsson et al., 2003). Because of the importance of resuspended organic material for the vertical mass flux and bioturbation, the annual variability in the organic matter composition at the sediment surface varies year-round only between 5 and 6 % OC with relatively constant C/N ratios between 7.9 and 9.1 at Station B1 and 8.3 and 9.2 at Station H6 (Bonaglia et al., 2014). Organic mass accumulation rates in the accumulation bottoms based on ^{210}Pb dating are reported between 3.3 and 9.5 mol m^{-2} y^{-1} (Thang et al., 2013; Karlsson et al., 2010). The combined effect of these sedimentation characteristics is that temporal variability in the settling primary organic carbon flux above the sediment surface is low, which reduces the overall temporal variability in organic carbon amount and composition and thereby in carbon mineralization rates. This small temporal variability is further influenced by macrofauna bioturbation in the top 2-3 cm of sediment in this area, foremost by the bivalve *Macoma baltica*, the arthropod *Pontoporeia femorata*, and the polychaete *Marenzelleria* (Bonaglia et al., 2014). Although macrofauna is largely absent at Station H6, sediment is also mixed at station H6 by bioturbating meiofauna (mostly ostracods) (Bonaglia et al., 2014).

The measured benthic oxygen uptake rates are consistent with the low variability in the surface organic carbon concentrations, C/N ratios, and a temperature-dependent decrease in total oxygen uptake rates in winter. The slightly higher total oxygen uptake rate at Station H6 is also consistent with the physiography of the enclosed small basin favouring sediment trapping of fine material. In addition, the location of station H6 in the inner fjärd limits water exchange and leads to greater oxygen depletion, whereas the more open station B1 is affected by upwelling of oxygen-rich waters and comparatively less burial of organic material (Table 1).

4.3 Methane fluxes, sulfate reduction and methane oxidation

Preferential accumulation of sediment in the bathymetric depressions of the inner Himmerfjärden results in very high sedimentation rates between 0.9 and 1.3 cm/yr (Thang et al., 2013; Bianchi et al., 2002). In such sediments organic carbon burial and transfer of organic matter into the methanogenic zone is efficient and will occur within 20 to 30 years. As a consequence of the low bottom water salinity of 6 ‰ of the Baltic Sea at this latitude, seawater sulfate concentrations are less than 7 mM and, by comparison with normal seawater, a comparatively lesser amount of organic matter can be degraded by bacterial sulfate reduction (Thang et al., 2013). Consequently, compared to normal marine sediments a larger proportion of organic matter undergoes anaerobic microbial degradation terminating in methanogenesis, which generates a high upward flux of methane into the sulfate-containing zone. Organiclastic sulfate-reducing bacteria will compete for the available sulfate with sulfate-reducing bacteria involved in the anaerobic oxidation of methane (Dale et al., 2006; Jørgensen and Parkes, 2010). Thermodynamic and kinetic constraints decide on the outcome between these two competing processes. Dale et al. (2006) suggested that due to lower winter temperatures and greater sulfate availability in the sulfate-methane transition zone in winter, the thermodynamic driving force for anaerobic methane oxidation increases allowing for a greater proportion of anaerobic methane oxidation coupled to sulfate reduction in the winter. In the summer and fall, higher temperatures and sulfate limitation may favor organiclastic sulfate reduction and methanogenesis while limiting the anaerobic oxidation of methane. Most importantly, however, their analysis showed that due to thermodynamic constraints and slow growth rates of the methane-oxidizing archaea the microbial biomass does not change significantly over a year. These conceptual modelling results can be tested with our Himmerfjärden data.

Sulfate reduction rates, particularly at H6, demonstrate how strongly bottom-water oxygen controls organic matter mineralization. In the spring, summer, and fall sulfate reduction was at its maximum in the first two centimeters of the sediments (Fig. 3 e, f, g). In February, reduced organic carbon input and

476 higher oxygen concentrations resulted in lower sulfate reduction rates and a downward displacement of
477 the maximum rates sediment confining methane production to greater depths in the sediment.
478 The decrease in oxygen uptake matches well with the decrease in methane fluxes at the two stations in
479 winter, which suggests an impact of oxygen on methane cycling (Table 2, Figure 5). Higher oxygen
480 levels enhance bioturbation and oxygen uptake by the abundant macro- and meiofauna (Norkko et al.,
481 2015), but the mixing of sediment also affects methane transport to the water column, as the main
482 transport process shifts from diffusion to advection. This effect is likely the main cause for the winter
483 decrease in methane fluxes and concentrations. More aerated conditions indirectly enhance methane
484 removal by sustaining aerobic methanotrophs (Valentine 2011). It is plausible that, as in other brackish
485 coastal sediments, aerobic methanotrophs at the surface of Himmerfjärden sediments consume a
486 significant part of upward-diffusing methane that was not oxidized by anaerobic methane oxidation
487 (McDonald et al 2005, Moussard et al 2009, Treude et al 2005a).
488 Published benthic methane fluxes for estuaries with similar salinities have a reported range of 0.002 to
489 0.25 mmol m^{-2} d^{-1} (Abril and Iversen, 2002; Martens and Klump, 1980; Sansone et al., 1998; Zhang et
490 al., 2008; Borges and April, 2012; Martens et al., 1998). The methane fluxes derived from our core
491 incubations (0.1-3.9 mmol m^{-2} d^{-1}, ignoring the potentially biased value of 19.9 mmol m^{-2} d^{-1}) and the
492 corresponding diffusive fluxes (0.01-2.4 mmol m^{-2} d^{-1}) were high compared to these published fluxes.
493 However, our fluxes are consistent with fluxes based on porewater gradients by Thang et al. (2013) that
494 were between 0.3 and 1.1 mmol m^{-2} d^{-1} at 3 nearby stations measured in May 2009.
495 A conspicuous property of all porewater profiles at station H6, with the exception of the February 2013
496 sampling period, was the absence of a curvature in most methane concentration profiles, which would
497 be expected for net methane oxidation by aerobic and anaerobic methane oxidation (Martens et al.,
498 1998). Most concentration profiles of sulfate and methane at Station H6 overlapped without a
499 significant change in the methane concentration gradient. A similar observation has been made earlier
500 for other Himmerfjärden sediments (Thang et al., 2013), and has also been reported for sediments of
501 the northwestern Black Sea shelf (Knab et al., 2009) and in organic-rich shelf sediment of the

Namibian upwelling system (Brüchert et al., 2009). Inefficient methane oxidation is also evident from the diffusive fluxes, which showed that the upward fluxes of methane into the sulfate-methane transition zone were only marginally higher than the methane fluxes to the sediment surface indicating little attenuation of the methane flux in the sulfate-methane transition zone (Table 2). One possible explanation for this phenomenon is therefore that rates of sulfate reduction–coupled anaerobic methane oxidation, except for the winter months, were low compared to the organiclastic sulfate reduction rate. An alternative explanation of our observations could be that the methane concentration gradients were affected by the presence of rising methane bubbles (Haeckel et al., 2007), or that bioturbation and bioirrigation linearized the concentration profiles (Dale et al., 2013). However, we do not favor these latter interpretations because of the absence of large macrofauna at station H6, the fact that methane concentrations were below the in-situ saturation concentration of methane, and the fast porewater methane sampling method preventing significant gas formation.

An analysis of the cumulative distribution of ^{35}S-SRR with depth at station H6 provides clues to the proportion of organoclastic relative to anaerobic methane oxidation-coupled sulfate reduction at Station H6 (Figure 6 e-h). In contrast to station B1, where an exponentially decreasing portion of sulfate reduction contributed to the total sulfate reduction at depth, at station H6 a distinct steepening in the cumulative sulfate reduction is observed below 10 cm in April, August, and October. As discussed above, we do not attribute the steepening observed in February 2013 to the same process, because sulfate was still present in abundance at this depth and methane conentrations were low and without any apparent change in gradient in this depth zone. The gradient in organoclastic sulfate reduction can be described by an exponential function (Jørgensen and Parkes, 2010),

$$^{35}SRR = y\, z^{-b} \quad (6)$$

where z is depth (cm) and y and b are regression coefficients (Jørgensen and Parkes, 2010). Fitting the sulfate reduction rates investigated here to such a function yielded exponential coefficients b between 0.4 and 0.9 at station B1 and 0.3 and 0.8 at Station H6 (Table 4). At Station H6 the lowest coefficient was found for February 2013, when sulfate penetrated the deepest into the sediment (Table 4). Since

528 the upward flux of methane provides an additional energy source to sulfate-reducing bacteria, total
529 sulfate reduction rates are expected to increase in the sulfate-methane transition zone. If substantial
530 AOM-coupled and organiclastic sulfate reduction occur at the same depths the total ^{35}S-sulfate
531 reduction rate depth gradient will be lower and the exponential coefficient b will be smaller than for a
532 setting without significant AOM. The difference between the exponential coefficients for the different
533 observation times can be used to calculate the variation in the contribution of AOM to the total sulfate
534 reduction rate. At station H6, between 5 % (August 2012) and 20% (April 2012) of the total sulfate
535 reduction can be associated with anaerobic methane oxidation. A comparison of the above method with
536 the ^{35}S-sulfate reduction rates integrated over the length of the H6 sediment cores with the rates
537 integrated in the AOM zone also indicated that >20% of sulfate reduction at H6 was supported by
538 anaerobic methane oxidation (Table 2). In near-shore continental margin sediments worldwide, the
539 fraction of methane-driven sulfate reduction varies between locations and accounts for 3-40% of total
540 sulfate reduction, with 10% possibly representing a global mean value (Jørgensen and Kasten, 2006).
541 The average 20% contribution calculated here falls in the upper range of these values and is similar to
542 values reported before for one of the monitoring stations within Himmerfjärden (Thang et al., 2013)
543 and also for a very productive Chilean slope sediment (8-24 %) (Treude et al 2005b). The good match
544 between the upward fluxes of methane in the sulfate-methane transition zone and the measured sulfate
545 reduction rates in the transition zone also indicate that other proposed electron acceptors for anaerobic
546 methane oxidation such as iron are unimportant in these sediments (Beal et al., 2009; Egger et al.
547 2014).
548
549 **4.4 Temporal variability in hydrostatic pressure**
550 The abrupt decrease in porewater methane concentrations from October 2012 to early February 2013
551 and the subsequent increase in April 2013 cannot be explained by variation in methane oxidation alone,
552 because the temporal change in porewater methane concentration was large compared to the inferred
553 methane oxidation rates based on fluxes in and out of the AOM zone. In addition, except for

554 downward-diffusing sulfate, there was no significant other electron acceptor present at depth. It is
555 unlikely that rates of methanogenesis would have decreased significantly between the fall and the
556 winter and resumed again in the spring because of the sedimentological characteristics described above
557 and the small difference in sediment temperatures for February and April (Table 1). Changes in organic
558 matter sedimentation at the sediment surface also have no significant influence on methanogenesis rates
559 in buried sediment and cannot explain the sudden decrease in methane concentration at depth. An
560 alternative explanation for the changes in methane concentrations is required. A possible explanation
561 could be that changes in upward transport of methane are due to variability in hydrostatic pressure and
562 the associated diffusive and advective upward transport of methane from depth. The free gas depth of
563 methane is thought to follow changes in hydrostatic pressure and temperature (Mogollon et al., 2011;
564 Toth et al., 2015). An estimated 10% of the fine-grained sediments in the Stockholm archipelago area
565 are underlain by pockets of free methane (Persson and Jonsson, 2000) and these free gas pockets are
566 preferentially located in areas with the thickest postglacial mud accumulation, generally in the center of
567 the sub-basins and along fault lineaments (Söderberg and Floden, 1992). Based on sub-bottom
568 echosounder profiling, the surface of the free gas zone in accumulation areas in Himmerfjärden and
569 other areas of the Stockholm archipelago is between 1 and 3 meter depth (Söderberg and Floden,
570 1991). During low sealevel stand the free gas zone is expected to migrate closer to the sediment
571 surface, whereas during high sealevel the free gas zone is depressed into the sediment. The total
572 variation in sealevel is related to air pressure, prevailing wind directions, precipitation, and the balance
573 of saltwater entry through the Danish straits and freshwater discharge from rivers entering the Baltic
574 Sea (Andersson, 2002). Additional effects are caused by local coastal bathymetry, current flow, and,
575 possibly, and local submarine groundwater discharge. These multiple parameters result in complex
576 subsurface hydrology and may produce sealevel fluctuations that can be as much as 50 cm, sufficient to
577 explain the changes in methane concentrations observed here. Unfortunately, local data within
578 Himmerfjärden on sealevel fluctuations are not available for our respective sampling locations, and
579 regional sealevel stands should not be directly applied to the sample sites.

The above discussion demonstrates that a variety of processes interact in these fjord sediments to produce the observed methane fluxes. It is beyond the scope of this paper to develop a unifying model against which the variability of the observed fluxes can be tested, but we would like to point out that the local coastal hydrography and hydrogeology would need to be accounted for in such a coupled physical biogeochemical model. To our knowledge, sufficient subsurface geophysical data are currently not available to establish appropriate physical boundary conditions for such a model. Detailed geophysical analysis of the subsurface structure at high vertical resolution together with long-term monitoring of the porewater chemistry would shed new light on the coupling between subsurface hydrology and methane emissions.

5 Conclusions

A greater understanding of methane emissions from estuarine and coastal sediments is important to estimate the contribution of these environments to global marine methane fluxes. High benthic fluxes of methane from these sediments showed that total methane oxidation was relatively inefficient, despite the fact that anaerobic methane oxidation contributed up to 20% to total sulfate reduction. Of the different environmental regulators, bottom water oxygen had the strongest influence for the regulation of methane emissions. Oxygen availability directly enhanced aerobic organic matter mineralization by shifting the redox cascade in the sediments and indirectly by stimulating meiofauna and macrofauna activity thereby stimulating both the aerobic carbon mineralization and oxidative recycling of sulfate. The annual variability in sediment methane concentrations and benthic methane fluxes indicate that the annual environmental changes at these near-shore, but relatively deep-water localities are considerable. Very few data on sediment biogeochemical processes are currently available for aerobic and anaerobic carbon mineralization and methane cycling during winter months when ice cover inhibits access and

sampling. Process rates inferred from sampling during open-water conditions over the whole year are therefore likely overestimates.

Hydrostatic pressure changes and complex subsurface hydrological conditions may also affect the temporal variability of subsurface methane concentrations. The spatial and temporal variability of these conditions must also be considered as an important component for understanding methane emissions from near-shore coastal and estuarine waters.

6. Author contribution

Joanna E. Sawicka conducted the sampling and analysis for the study and wrote the manuscript. Volker Brüchert devised the study, interpreted the data, created the figures and tables, and wrote the manuscript.

7. Data availability

The data are available from the second author upon request.

8. Acknowledgments

We are grateful to the staff of Askö Laboratory for their help and cooperation during the cruises and our stays on the island of Askö. We would like to thank Barbara Deutsch, Camilla Olsson and Stefano Bonaglia for their help during sampling. The study was funded by the grant from the Bolin Centre for Climate Research, Baltic Ecosystem Adaptive management (BEAM), and the EU BONUS project Baltic Gas. We acknowledge the comments by two reviewers that substantially changed the manuscript.

References

Abril, G. and Iversen, N.: Methane dynamics in a shallow non-tidal estuary (Randers Fjord, Denmark), Mar Ecol Prog Ser, 230, 171-181, 2002.

Amouroux, D., Roberts, G., Rapsomanikis, S. and Andreae, M.O.: Biogenic gas (CH_4, N_2O, DMS) emission to the atmosphere from near-shore and shelf waters of the North-western Black Sea, Estuar Coast Shelf S, 54, 575-587, 2002.

Bange, H. W., Bergmann, K, Hansen, H. P., Kock, A., Koppe, R., Malien, F., Ostrau, F., Dissolved methane during hypoxic events at the Boknis Eck time series station (Eckernförde Bay, SW Baltic Sea), Biogeosciences, 7, 1279-1284, 2010.

Beal, E. J., House, C. H., Orphan, V. J.: Manganese- and Iron-Dependent Marine Methane Oxidation, Science 325, 184-187, 2009.

Bianchi, T. S., Engelhaupt, E., McKee B. A., Miles, S., Elmgren, R., Hajdu, S., Savage, C., and Baskaran, M.: Do sediments from coastal sites accurately reflect time trends in water column phytoplankton? A test from Himmerfjärden Bay (Baltic Sea proper), Limnol. Oceanogr., 47, 1537-1544, 2002.

Blomqvist, S. and Larsson, U.: Detrital bedrock elements as tracers of settling resuspended particulate matter in a coastal area of the Baltic Sea, Limnol. Oceanogr., 39, 880-896, 1994.

Boesch, D. F., Hecky, R., O'Melia, C., Schindler, D., Seitzinger, S.: Eutrophication of the Swedish Seas, Reports of the Swedish Environmental Protection Agency, Stockholm, Sweden, No. 5509, 72 p, 2006.

Bonaglia, S., Bartoli, M., Gunnarsson, J. S., Rahm, L., Raymond, C., Svensson, O., Shakeri, Brüchert, V.: Effect of reoxygenation and Marenzelleria spp. bioturbation on Baltic Sea sediment metabolism, Marine Ecology Progress Series, 482, 43-55, 2013.

Bonaglia, S., Deutsch, B., Bartoli, M., Marchant, H. K. and Brüchert, V.: Seasonal oxygen, nitrogen and phosphorus benthic cycling along an impacted Baltic Sea estuary: regulation and spatial patterns, Biogeochemistry, 119, 1-22, 2014.

Borges, A. V. and Abril, G.: Carbon Dioxide and Methane Dynamics in Estuaries, in: Treatise on Estuarine and Coastal Science, (Eds.) Wolanski, E., McLusky, D., Academic Press, Waltham, 119-161, 2011.

Boudreau, B.P.: Diagenetic models and their implementation. Springer Verlag, Berlin Heidelberg, 1996.

Brüchert, V., Currie, B., Peard, K.: Hydrogen sulphide and methane emissions on the central Namibian shelf, Progr. Oceanogr., 83, 169-179, 2009.

Crill, P. M. and Martens, C. S.: Spatial and temporal fluctuations of methane production in anoxic coastal marine sediments, Limnol. Oceanogr., 6, 1117-1130, 1983.

Dale, A. W., Regnier, P., Van Cappellen, P.: Bioenergetic Controls on Anaerobic Oxidation of Methane (AOM) in Coastal Marine Sediments: A Theoretical Analysis, Am. J. Sci., 306, 246-294, 2006.

Dale, A. W., Aguilera, D. R., Regnier, P., Fossing, H., Knab, N. J., Jørgensen, B. B.: Seasonal dynamics of the depth and rate of anaerobic oxidation of methane in Aarhus Bay (Denmark) sediments, J. Mar. Res., 66, 127-155, 2008.

Dale, A. W., Bertics, V. J., Treude, T., Sommer, S., Wallmann, K.: Modeling benthic–pelagic nutrient exchange processes and porewater distributions in a seasonally hypoxic sediment: evidence for massive phosphate release by Beggiatoa? Biogeosciences, 10, 629-651, 2013.

Egger, M., Rasigraf, O., Sapart, C. J., Jilbert, T., Jetten, M. S. M., Röckmann, T.: Iron-mediated anaerobic oxidation of methane in brackish coastal sediments, Env. Sci. Technol., 49, 277-283, 2014.

Elmgren, R. and Larsson, U.: Himmerfjärden: förändringar i ett näringsbelastat kustekosystem i Östersjön, Reports of the Swedish Environmental Protection Agency, Stockholm, Sweden, 1997.

Engqvist, A., Long-term nutrient balances in the eutrophication of the Himmerfjärden, Estuar. Coast. Shelf S., 42, 483-507, 1996.

Giuseppe Etiope, G., Lassey, K.R., Klusman, R.W., Boschi, E.: Reappraisal of the Fossil Methane Budget and Related Emission from Geologic Sources, Geophys. Res. Lett., 35, ISSN 1944-8007, 2008.

Haeckel, M., Boudreau, B. P., Wallmann, K.: Bubble-induced porewater mixing: A 3-D model for deep porewater irrigation, Geochim Cosmochim, Acta, 71, 5135-5154, 2007.

Harvey, E. T., Kratzer, S., Philipson, P.: Satellite-based water quality monitoring for improved spatial and temporal retrieval of chlorophyll-a in coastal waters, Remote Sens. Environ., 158, 417-430, 2015.

Iversen, N., Jørgensen, B. B.: Diffusion coefficients of sulfate and methane in marine sediments: Influence of porosity, Geochim. Cosmochim. Acta 57, 571-578, 1994.

Jørgensen, B. B. and Kasten, S.: Sulfur Cycling and Methane Oxidation, In: Marine Geochemistry, (Eds.) Schulz H. and Zabel, M., Springer, Berlin Heidelberg, 271-309, 2006.

Jørgensen, B. B.: A comparison of methods for the quantification of bacterial sulfate reduction in coastal marine sediments, Geomicrobiol. J., 1, 11-27, 1978.
Jørgensen, B. B. and Parkes, R. J.: Role of sulfate reduction and methane production by organic carbon degradation in eutrophic fjord sediments (Limfjorden, Denmark), Limnol. Oceanogr., 55, 1338-1352, 2010.
Jonsson, P., Persson, J., Holmberg, P.: Skärgårdens bottnar, Report of the Swedish Environmental Protection Agency, Stockholm, No. 5212, 114, 2003.
Judd, A. G.: Natural seabed gas seeps as sources of atmospheric methane, Environ. Geol., 46, 988-996, 2004.
Kallmeyer, J., Ferdelman, T. G., Weber, A., Fossing, H., Jørgensen, B. B.: Evaluation of a cold chromium distillation procedure for recovering very small amounts of radiolabeled sulfide related to sulfate reduction measurements, Limnol. Oceanogr. Meth., 2, 171-180, 2004.
Kampbell, D. H., Wilson, J. T., Vandegrift, S. A.: Dissolved Oxygen and Methane in Water by a GC Headspace Equilibration Technique, Intern. J. Environ. An. Ch., 36, 249-257, 1989.
Karlsson, M., M. Malmaeus, M., Rydin, E., Jonsson, P.: Bottenundersökningar i Upplands, Stockholms, Södermanlands och Östergötlands skärgårdar: 2008-2009. Svenska Miljöinstitut, B1928, 102, 2010.
King, G.M.: Ecological Aspects of Methane Oxidation, a Key Determinant of Global Methane Dynamics, In: Advances in Microbial Ecology, 12, Marshall, K.C. (ed.), 431-468, 1992.
Kirschke, S., Bousquet, P., Ciais, P., Saunois, M., Canadell, J.G., Dlugokencky, E.J., Bergamaschi, P., Bergmann, D., Blake, D.R., Bruhwiler, L.: Three Decades of Global Methane Sources and Sinks, Nat. Geosci., 6, 813-23, 2013.
Knab, N. J., Cragg, B. A., Borowski, C., Parkes, R. J., Pancost, R. and Jørgensen, B. B.: Anaerobic oxidation of methane (AOM) in marine sediments from the Skagerrak (Denmark): I. Geochemical and microbiological analyses. Geochim. Cosmochim. Acta, 72, 2868-2879, 2009.
Knittel, K. and Boetius, A.: Anaerobic Oxidation of Methane: Progress with an Unknown Process. Ann. Rev. Microbiol., 63: 311-334, 2009.
Klump, J. V. and Martens, C. S.: Biogeochemical cycling in an organic rich coastal marine basin—II. Nutrient sediment-water exchange processes. Geochim. Cosmochim. Acta, 45, 101-121, 1981.
Kristensen, E., Bouillon, S., Dittmar, T., Marchand, C.: Organic carbon dynamics in mangrove ecosystems: A review. Aquat. Bot., 89, 201-219, 2008.
Larsson, U., Nyberg, U., Höglander, H., Sjösten, A., Sandberg, M., Walve, J.: Himmerfjärdens miljörapport 2012, Department of Ecology, Environment, and Plant Sciences, Technical Report 50, 75, 2012.
Leloup, J., Fossing, H., Kohls, K., Holmkvist, L., Borowski, C., Jørgensen, B. B.: Sulfate-reducing bacteria in marine sediment (Aarhus Bay, Denmark): abundance and diversity related to geochemical zonation. Environ. Microbiol., 11, 1278-1291, 2009.
Martens, C. S., Albert, D. B., Alperin, M. J.: Biogeochemical processes controlling methane in gassy coastal sediments - Part 1. A model coupling organic matter flux to gas production, oxidation, and transport. Cont. Shelf Res., 18, 1741-1770, 1998.
Martens, C. S. and Berner, R. A.: Methane production in the interstitial waters of sulfate-depleted marine sediments. Science, 185, 1167-1169, 1974.
Martens, C. S. and Klump, J.: Biogeochemical cycling in an organic-rich coastal marine basin. 4. An organic carbon budget for sediments dominated by sulfate reduction and methanogenesis. Geochim. Cosmochim. Acta, 48, 1987-2004, 1984.
Martens, C.S. and Val Klump, J.: Biogeochemical cycling in an organic-rich coastal marine basin—I. Methane sediment-water exchange processes. Geochim. Cosmochim. Acta, 44, 471-490, 1980.
Marty, D., Bonin, P., Michotey, V. and Bianchi, M.: Bacterial biogas production in coastal systems affected by freshwater inputs. Cont. Shelf Res., 21, 2105-2115, 2001.
McDonald, I. R., Smith, K., Lidstrom, M. E.: Methanotrophic populations in estuarine sediment from Newport Bay, California, FEMS Microbiol. Lett., 250, 287-293, 2005.
Middelburg, J., Nieuwenhuize, J., Iversen, N., Høgh, N., de Wilde, H., Helder, W., Seifert, R. and Christof, O.: Methane distribution in European tidal estuaries, Biogeochemistry, 59, 95-119, 2002.
Mogollón, J. M., Dale, A. W., L'Heureux, I., Regnier, P.: Impact of seasonal temperature and pressure changes on methane gas production, dissolution, and transport in unfractured sediments, J. Geophys. Res. Biogeosci., 116, G03031, 2011.
Moussard, H., Stralis-Pavese, N., Bodrossy, L., Neufeld, J. D., Murrell, J. C.: Identification of active methylotrophic bacteria inhabiting surface sediment of a marine estuary, Environ. Microbiol. Repts., 1, 424-433, 2009.
Musenze, R.S., Werner, U., Grinham, A., Udy, J. and Yuan, Z.: Methane and nitrous oxide emissions from a subtropical estuary (the Brisbane River estuary, Australia), Sci. Total Environ., 472, 719-729, 2014.

Nguyen, T.D., Crill, P. and Bastviken, D.: Implications of temperature and sediment characteristics on methane formation and oxidation in lake sediments, Biogeochemistry 100, 185-196, 2010.
Norkko, J., Gammal, J., Hewitt, J., Josefson, A., Carstensen, J., Norkko, A.: Seafloor Ecosystem Function Relationships: In Situ Patterns of Change Across Gradients of Increasing Hypoxic Stress, Ecosystems 18, 1424-1439, 2015.
Persson, J., Jonsson, P.: Historical development of laminated sediments–an approach to detect soft sediment ecosystem changes in the Baltic Sea. Mar. Poll. Bull., 40, 122-134, 2000.
Reeburgh, W. S.: Oceanic Methane Biogeochemistry, Chem. Rev., 107, 486-513, 2007.
Reindl, A. R. and Bolałek, J.: Methane flux from sediment into near-bottom water and its variability along the Hel Peninsula—Southern Baltic, Sea, Cont. Shelf Res., 74, 88-93, 2014.
Savage, C., Leavitt, P. R., Elmgren, R.: Effects of land use, urbanization, and climate variability on coastal eutrophication in the Baltic Sea. Limnol. Oceanogr., 55, 1033-1046, 2010.
Sansone, F. J., Holmes, M. E. and Popp, B. N.: Methane stable isotopic ratios and concentrations as indicators of methane dynamics in estuaries. Global Biogeochem. Cycles, 13, 463-474, 1999.
Sansone, F. J., Rust, T. M. and Smith, S. V., 1998. Methane Distribution and Cycling in Tomales Bay, California, Estuaries, 21, 66-77.
Seeberg-Elverfeldt, J., Schlüter, M., Feseker, T., Kölling, M.: Rhizon sampling of porewaters near the sediment-water interface of aquatic systems. Limnol. Oceanogr. Meth., 3, 361-371, 2005.
Smith, R.W., Bianchi, T.S., Allison, M., Savage, C., Galy, V.: High rates of organic carbon burial in fjord sediments globally. Nature Geosci., 8, 450-453, 2015.
Söderberg, P. and Flodén, T.: Gas seepages, gas eruptions and degassing structures in the seafloor along the Strömma tectonic lineament in the crystalline Stockholm Archipelago, east Sweden. Cont. Shelf Res. 12, 1157-1171, 1992.
Stridh, S.: SYVAB Himmerfjärdsverket Miljörapport 2012, www.syvab.se/information/dokument/syvabs-miljorapporter, 53, 2012.
Thang, N., Brüchert, V., Formolo, M., Wegener, G., Ginters, L., Jørgensen, B. B., and Ferdelman, T.: The Impact of Sediment and Carbon Fluxes on the Biogeochemistry of Methane and Sulfur in Littoral Baltic Sea Sediments (Himmerfjärden, Sweden), Estuaries and Coasts, 36, 98-115, 2013.
Tóth, Z., Spiess, V., Keil, H.: Frequency dependence in seismoacoustic imaging of shallow free gas due to gas bubble resonance, J. Geophys. Res. Solid Earth, 120, 8056-8072, 2015.
Treude, T., Krüger, M., Boetius, A., Jørgensen, B. B.: Environmental control on anaerobic oxidation of methane in the gassy sediments of Eckernförde Bay (German Baltic), Limnol. Oceanogr., 50, 1771-1786, 2005a.
Treude, T., Niggemann, J., Kallmeyer, J., Wintersteller, P., Schubert, C. J., Boetius. A., and Jørgensen, B. B.: Anaerobic oxidation of methane and sulfate reduction along the Chilean continental margin, Geochim. Cosmochim. Acta, 69, 2767-2779, 2005b.
Upstill-Goddard, R. C., Barnes, J., Frost, T., Punshon, S. and Owens, N. J. P.: Methane in the southern North Sea: Low-salinity inputs, estuarine removal, and atmospheric flux, Global Biogeochem. Cycles, 14, 1205-1217, 2000.
Valentine, D.L.: Emerging Topics in Marine Methane Biogeochemistry. Annual Rev. Mar. Sci., 3, 147-171, 2011.
Wegener, G., Bausch, M., Holler, T., Thang, N. M., Prieto Mollar, X., Kellermann, M. Y., Hinrichs, K. U., and Boetius, A.: Assessing sub-seafloor microbial activity by combined stable isotope probing with deuterated water and ^{13}C-bicarbonate. Environ. Microbiol., 14, 1517-1527, 2012.
Westrich, J. T., Berner, R. A.: The role of sedimentary organic matter in bacterial sulfate reduction: The G model tested. Limnol. Oceanogr., 29, 236-249, 1984.
Wik, M., Thornton, B.F., Bastviken, D., MacIntyre, S., Varner, R.K. and Crill, P.M.: Energy input is primary controller of methane bubbling in subarctic lakes. Geophysical Research Letters 41, 555-560, 2014.
Wilhelm, E., Battino, R., and Wilcock, R. J.: Low-pressure solubility of gases in liquid water. Chem. Rev., 77, 219-262, 1977.
Zakrisson, A., and Larsson, U.: Regulation of heterocyst frequency in Baltic Sea Aphanizomenon sp., J. Plankton Res., 36, 1357-1367, 2014.
Zhang, G., Zhang, J., Liu, S., Ren, J., Xu, J. and Zhang, F.: Methane in the Changjiang (Yangtze River) estuary and its adjacent marine area: riverine input, sediment release and atmospheric fluxes. Biogeochemistry, 91, 71-84, 2008.
Zhang, W., Bougouffa, S., Wang, Y., Lee, O. O., Yang, J., Chan C. Song, X., and Qian, P.-Y.: Toward understanding the dynamics of microbial communities in an estuarine system, PLoS ONE, 9, e94449, 2014.

788 **Table 1**. Main site characteristics of the sampling stations.

Station	Sampling time	Water depth (m)	Temperature (°C)	Bottom water salinity (‰)	Bottom water Oxygen (µM)	Surface organic carbon (%)
B1 58°48'18''N 17°37'52''E	April 2012	41	2.4	6.5	160	6.0
	August 2012		6.9	7.0	260	5.2
	October 2012		6.8	7.0	224	5.1
	February 2013		3.4	7.0	380	5.0
H6 59°04'08''N 17°40'63''E	April 2012	39.5	1.8	5.9	40	4.6
	August 2012		6.7	6.4	150	5.1
	October 2012		9.4	6.5	191	5.2
	February 2013		1.8	5.4	300	4.7

789

790

791

792

793

794

795

796

797 **Table 2.** Summary of CH_4 and SO_4^{2-} fluxes, depth-integrated ^{35}SRR, and total oxygen uptake (TOU).

Station	Sampling time	Flux (mmol m^{-2} d^{-1})						
		TOU whole core incubation (n=4)	**CH_4** whole core incubation (n=4)	**CH_4** Diffusive flux to sediment surface (n=1)	**CH_4** Diffusive flux into SMTZ (n=1)[2]	**SO_4^{2-}** Diffusive flux into sediment (n=1)	**^{35}S-SRR integrated over AOM[3] zone (n=3)**	**Integrated ^{35}S-SRR (n=3)**
B1	April 2012	19.7±2.5	-0.10±0.05	-0.1		0.4	no AOM zone[4]	2.3±0.6
	August 2012	22.5±2.9	-1.2±0.6	-(0.01)		0.8	no AOM zone[4]	0.5±0.1
	October 2012	21.1±2.7	No data	-0.3		1.4	no AOM zone[4]	2.0±0.0.5
	February 2013	12.0±1.5	-0.1±0.05	-0.02		0.2	no AOM zone[4]	2.2±0.6
H6	April 2012 April 2013	33.5±3.5	-0.3±0.1 -3.9 ±0.7[1]	-1.7	-2.8	2.6	(10-18 cm) = -2.8±0.7	11.6±2.9
	August 2012	26.9±2.8	-19.9±7.8[5]	-2.3	-2.6	2.7	(10-18 cm) = -2.8±0.7	11.7±2.9
	October 2012	25.9±2.7	-1.0	-2.0	-1.9	2.6	(10-18 cm) = -2.4±0.6	11.5±2.9
	February 2013	14.9+1.6	-1.1	-0.5	-0.4	1.3	no AOM zone[3]	9.2±2.3

798 [1] whole core incubation was performed in April 2013; Diffusive fluxes were calculated for samples collected in April 2012;
799 [2] SMTZ - sulfate methane transition zone, [3]AOM zone – zone of anaerobic oxidation of methane, [4] no AOM zone means
800 that AOM zone was probably deeper than the core length; [5] potentially elevated due to depressurization/ex-solution
801 effect during core incubation at atmospheric pressure;

802

803 **Table 3.** Best-fit regression coefficients a and b for the depth gradient of sulfate
804 reduction rates ($^{35}SRR = az^{-b}$ (z =depth, cm)).

Station	Sampling time	Exponential coefficient (a)	Exponential coefficient (b)
B1	April 2012	147.0	-1.4
	August 2012	11.7	-0.9
	October 2012	16.0	-0.4
	February 2013	33.5	-0.8
H6	April 2012	18.6	-0.5
	August 2012	37.4	-0.5
	October 2012	133.2	-0.8
	February 2013	25.0	-0.4

805

806

807

808

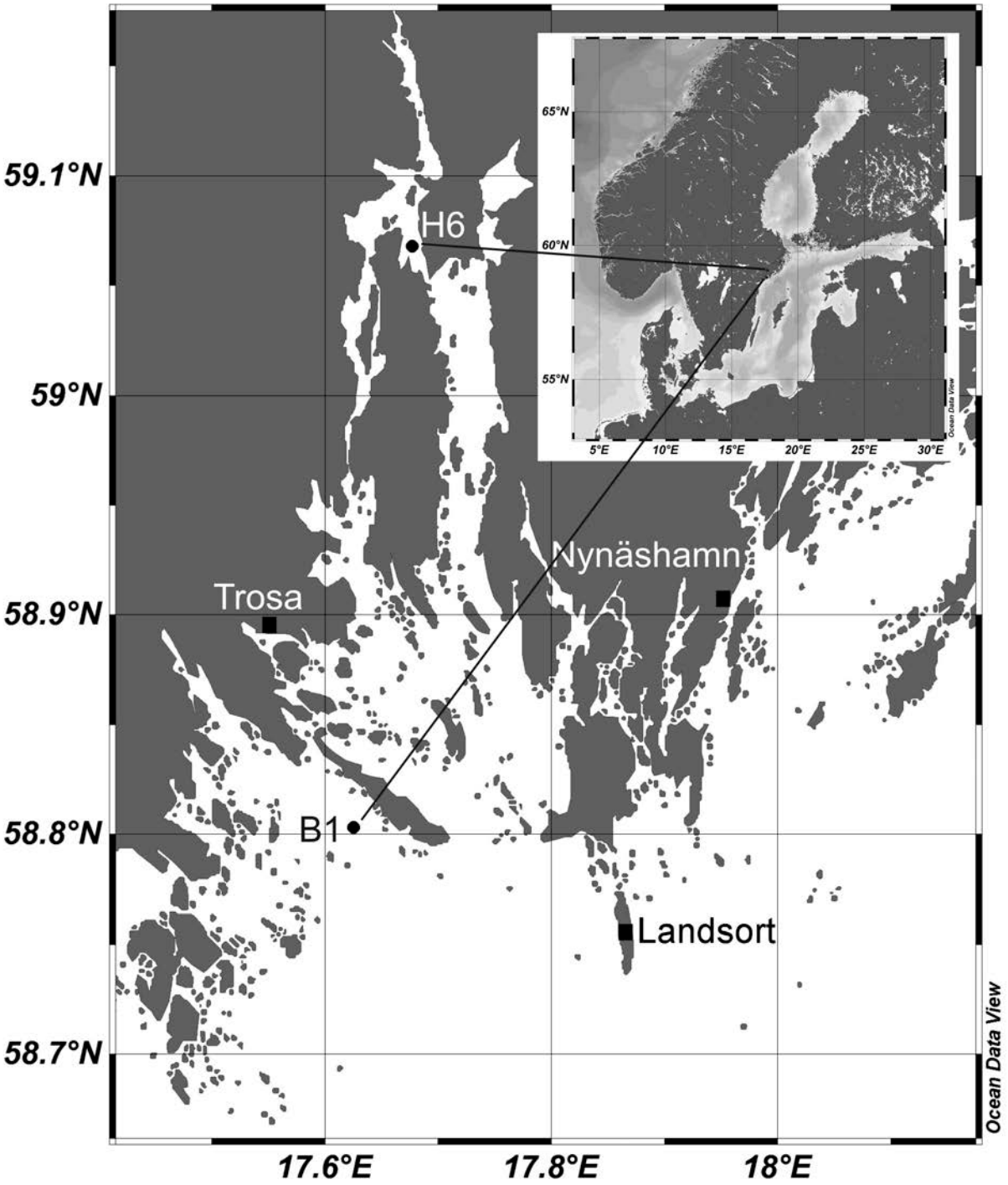

809

Figure 1. Location of sampling sites in Himmerfjärden, Stockholm Archipelago, Sweden. Detailed studies were conducted at two sites, an open water site (station B1) and in the inner part of the estuary (station H6).

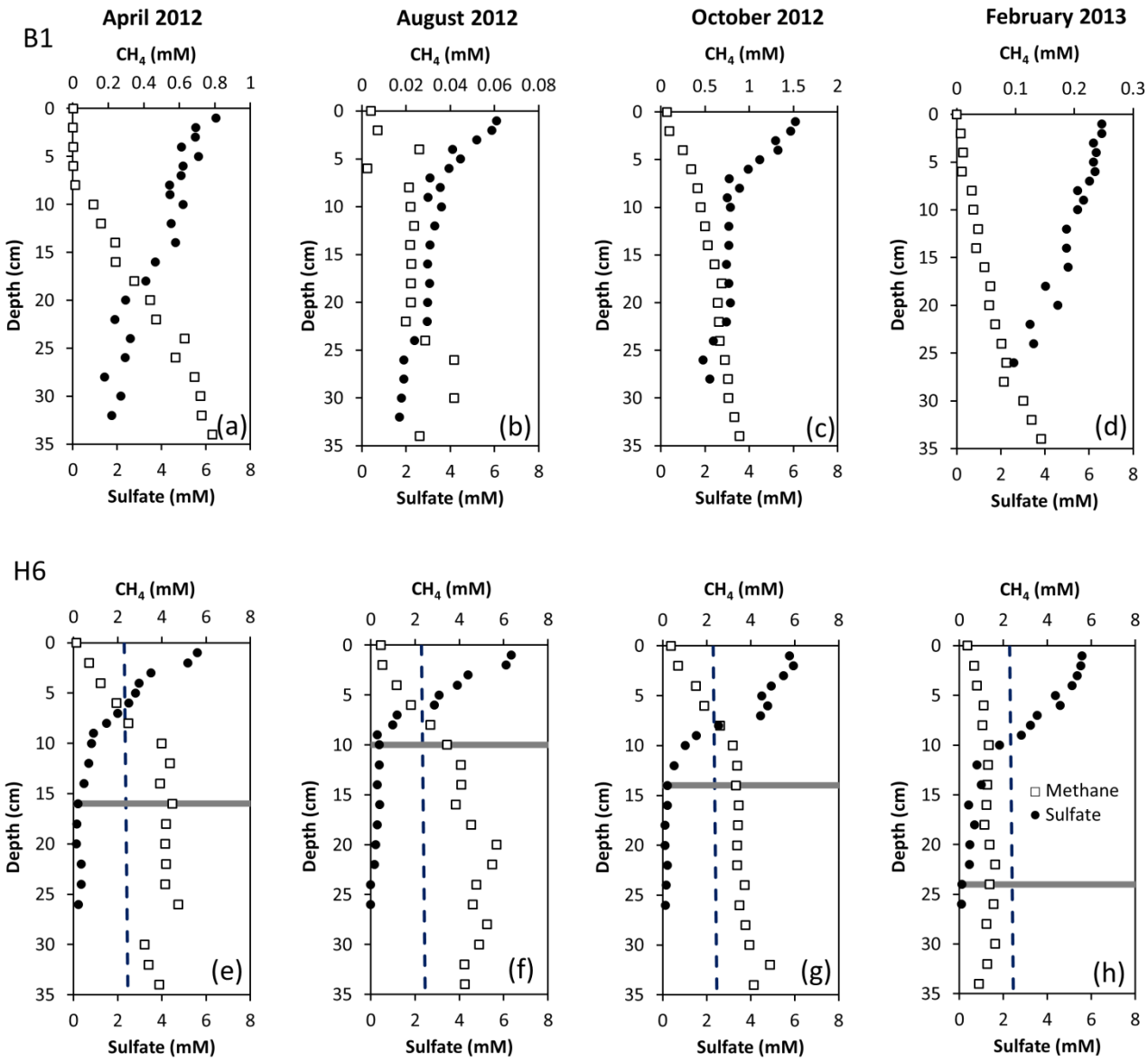

Figure 2. Porewater profiles of total methane and sulfate at Station B1 (a-d) and Station H6 (e-h) for the different sampling periods. The grey line marks the initial minimum sulfate concentration depth. Dashed lines indicate the methane saturation concentration at 1 atm pressure (grey) at the time of sampling. All concentrations of methane are below the in situ saturation concentration of methane (see text for details).

812

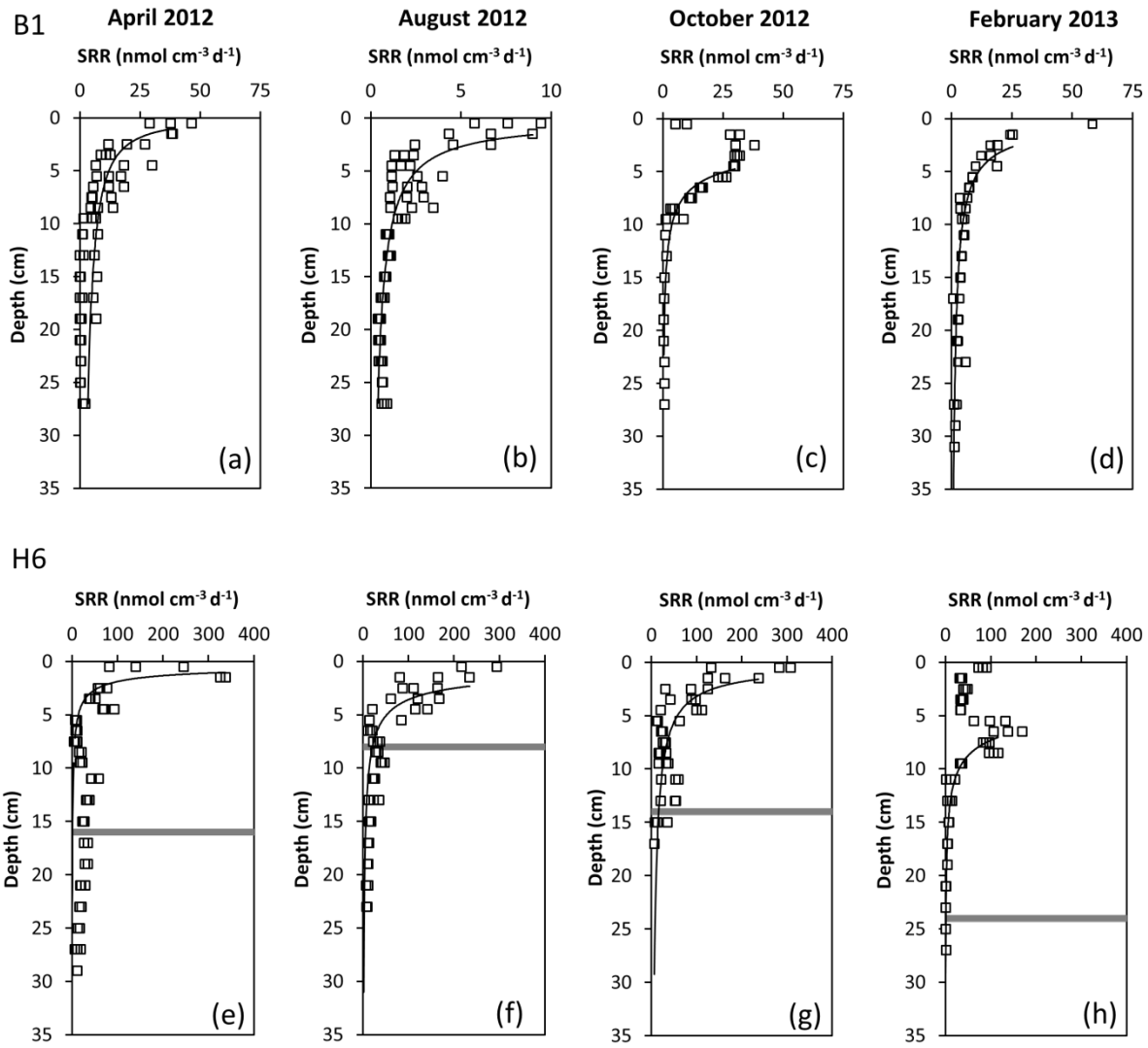

813

814

Figure 3. Depth gradients of bacterial sulfate reduction rates (SRR) measured with ^{35}S-sulfate at Station B1 (a-d) and Station H6 (e-h) for the different sampling periods. Black lines show the regression results to a power function of the form $y = ax^{-b}$. The grey line marks the initial minimum sulfate concentration depth.

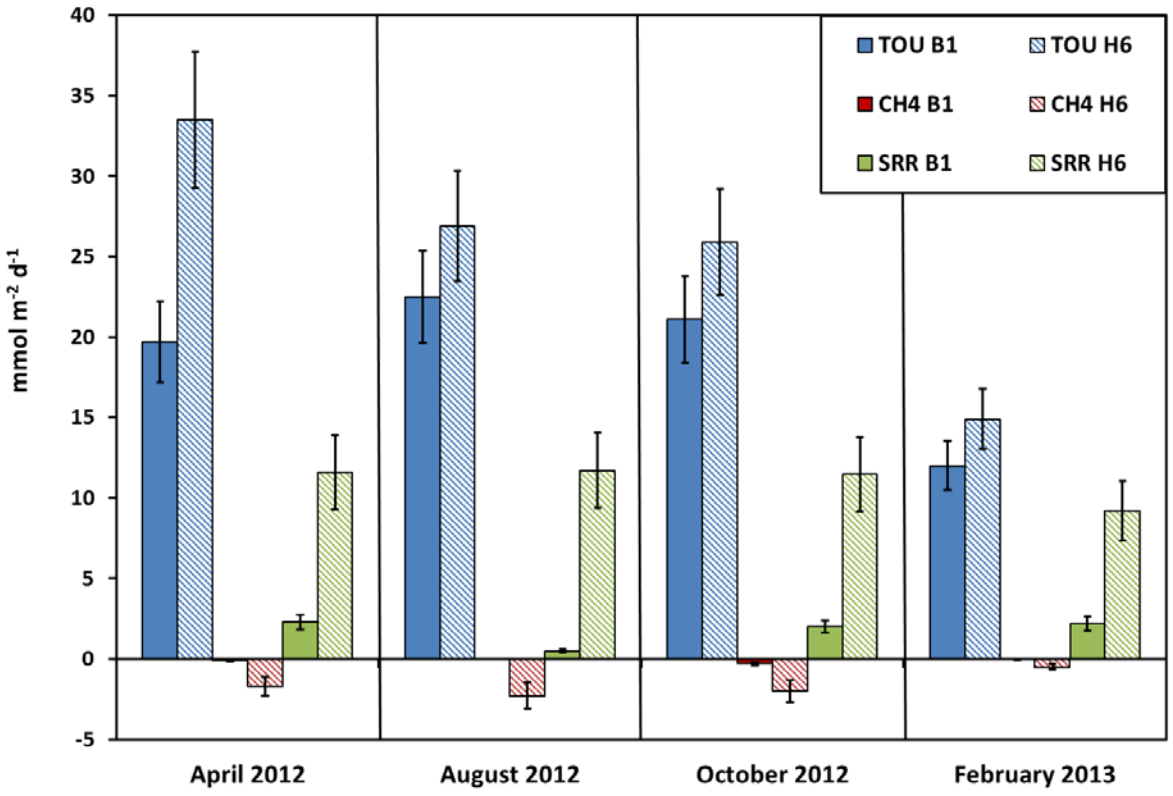

Figure 4. Comparison of benthic fluxes (mmol m^{-2} d^{-1}) for sulfate (SO_4), methane (CH_4), and oxygen (TOU) for the different sampling periods.

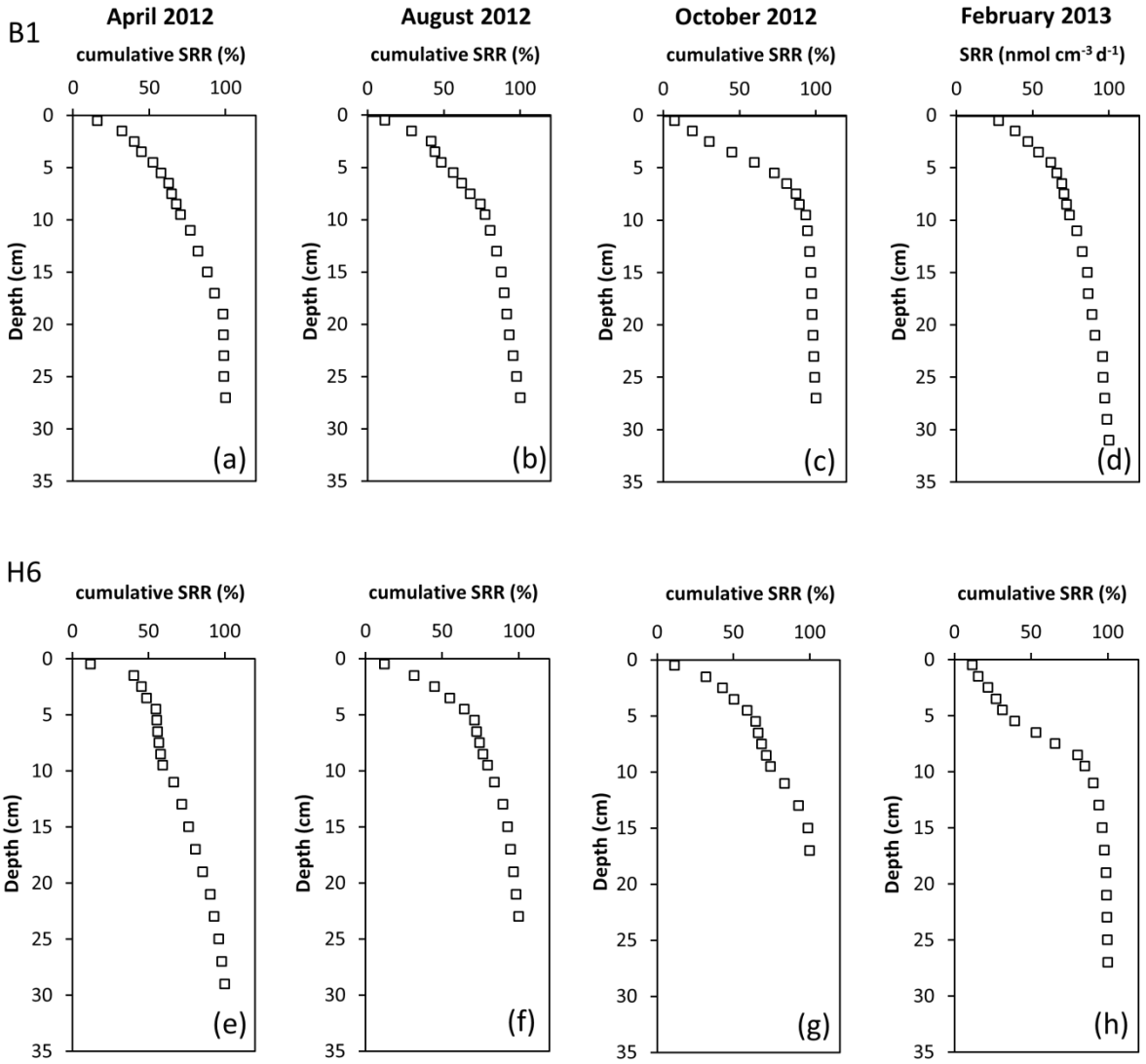

817

Figure 5. Depth distribution of sulfate reduction rate expressed as cumulative percentage at Station B1 (a-d) and Station H6 (e-h) for the different sampling periods. The grey line marks the initial minimum sulfate concentration depth.